Title

ISOBARIC ANALOGUE STATES AND COULOMB DISPLACEMENT ENERGIES IN THE (ld5/2) SHELL

Authors

Hardy, J.C.
Brunnader, H.
Cerny, Joseph
et al.

Publication Date

1969

UCRL-18566

cy. 2

ISOBARIC ANALOGUE STATES AND COULOMB DISPLACEMENT ENERGIES IN THE ($1d_{5/2}$) SHELL

J. C. Hardy, H. Brunnader,
Joseph Cerny, and J. Jänecke

January 1969

LAWRENCE RADIATION LABORATORY
UNIVERSITY of CALIFORNIA BERKELEY

cy. 2

UCRL-18566

DISCLAIMER

To be sumitted to: The Physical Review

UCRL-18566
Preprint

UNIVERSITY OF CALIFORNIA

Lawrence Radiation Laboratory
Berkeley, California

AEC Contract No. W-7405-eng-48

ISOBARIC ANALOGUE STATES AND COULOMB DISPLACEMENT ENERGIES IN THE $(1d_{5/2})$ SHELL

J. C. Hardy,[a] H. Brunnader,[b] Joseph Cerny,[a] and J. Jänecke[c]

January 1969

ISOBARIC ANALOGUE STATES AND COULOMB DISPLACEMENT ENERGIES IN THE ($1d_{5/2}$) SHELL*

J. C. Hardy, H. Brunnader, Joseph Cerny
Lawrence Radiation Laboratory and
Department of Chemistry
University of California
Berkeley, California

and

J. Jänecke
Department of Physics, University of Michigan
Ann Arbor, Michigan

January 1969

ABSTRACT

The (p,t) and (p,^{3}He) reactions have been used to locate three previously unknown T = 3/2 isobaric analogue states in ^{19}F, ^{19}Ne and ^{23}Mg, in addition to significantly improving the precision on the energies of the T = 3/2 state in ^{23}Na and the T = 2 states in ^{20}F and ^{24}Na. Including these data, twenty-eight displacement energies are now known throughout the ($1d_{5/2}$) shell for all possible multiplets with $T \leq 2$ (except T = 2, mass-22). The experimental displacement energies were compared in detail with calculations which used Hecht's Coulomb energy equations; the excellent agreement obtained appeared to be relatively insensitive to the assumed nuclear wave functions since both the low-seniority j-j coupling limit and the Wigner supermultiplet scheme produced similar results. Four parameters related to the two-body Coulomb-

energy matrix elements were treated as adjustable in fitting the data but their final values are in reasonable agreement with matrix elements calculated using harmonic oscillator wave functions. A fifth adjustable parameter took account of the Z- and N- dependence of the charge radius. Using the "best-fit" parameters the unmeasured masses of ^{19}Na, ^{20}Mg, ^{21}Mg, ^{22}Al, ^{23}Al, ^{24}Si and ^{25}Si are predicted, together with the excitation energies of unobserved analogue states in the $(1d_{5/2})$ shell.

I. INTRODUCTION

The success of the isobaric-multiplet mass-equation in relating the masses of states within a multiplet has been remarkable.[1] It is now clear that if there are any deviations from its quadratic form they will probably be small, and their detection over a range of multiplets would require an experimental precision which is not yet possible. However, in first order perturbation theory any charge-dependent force of tensorial rank of two or less (two-body forces usually have these characteristics) will give rise to such a quadratic mass formula. Deviations from the quadratic form may be expected if a first order perturbation treatment is not adequate. In order to examine the effects of non-Coulomb charge-dependent forces, the most valuable data would concern the variation of the coefficients in the quadratic mass formula as functions of mass number (A) and isospin (T). Since the Coulomb interaction is well understood, this (A,T) dependence can in principle be calculated under the assumption that the only charge-dependent forces are the Coulomb forces. One has to ascertain though that proper nuclear wave functions and charge radii are used and that higher order perturbations are either small or properly taken into consideration. The latter may affect the quadratic term considerably.[2] Any experimental deviation from such detailed calculations may then be interpreted as being due to non-Coulomb forces such as charge-dependent nuclear forces or forces resulting from the electromagnetic spin-orbit interaction.

In order to minimize the number of extraneous effects, it appeared desirable to carry out such an investigation within the confines of a single shell, and to discuss only the displacement energies (i.e. the energy differences between adjacent members of a multiplet) thus eliminating most of the effects of the nucleons in the core. We chose the $(1d_{5/2})$-shell since, including the six measurements reported here, displacement energies are known within multiplets over the full range of possible A's for all values of $T \leq 2$ with a single exception - the $T = 2$ multiplet in mass-22. This makes the $(1d_{5/2})$-shell more favorable than the $(1f_{7/2})$-shell, which has been extensively investigated previously,[3-6] because the former includes more measured displacement energies, they are known to greater precision and completely cover the mass region for many values of T.

We report the location of three previously unobserved $T = 3/2$ analogue levels in ^{19}F, ^{19}Ne and ^{23}Mg, in addition to significantly improving the precision on the energy of the $T = 3/2$ state in ^{23}Na and the $T = 2$ states in ^{20}F and ^{24}Na. These results are combined with all relevent experimental data previously obtained to produce twenty-eight displacement energies throughout the shell.

In the past, some analyses of Coulomb-displacement energies[5,6] have used the Coulomb energy formula of Carlson and Talmi.[7,8] This has met with surprising success considering that the formula was originally derived for proton configurations only and, as applied to n-nucleon systems of protons and neutrons, should only be valid if the seniority of the protons is a good quantum number. Recently, by considering the total isospin as a good quantum number, Hecht has derived Coulomb energy formulae which apply specifically

to a system of n neutrons and protons. These formulae have been derived in two limiting coupling-schemes: the j-j coupling low-seniority scheme[9] and the Wigner supermultiplet scheme.[10] In both schemes, the formulae have a similar form, and it might be anticipated that they should apply in any intermediate coupling scheme as well. They are expressed in terms of matrix elements which we will parameterize, the five parameters being determined from a fit to the experimental data. The values so obtained will subsequently be compared with calculations which used harmonic oscillator wave functions.

Such methods have already been applied with considerable success to the $(1f_{7/2})$ shell[3] but only formulae for the seniority scheme were used. The present analysis of the $(1d_{5/2})$-shell also provides the first examination of the importance of the coupling scheme assumed. The formulae are quite successful in fitting the experimental displacement energies. They can therefore be used with confidence to predict masses of unmeasured neutron-deficient nuclei and excitation energies of unobserved analogue states in the $(1d_{5/2})$ shell. Such predictions will be tabulated.

II. EXPERIMENTAL PROCEDURE

All measurements reported here were made using the external 45 MeV proton beam from the Berkeley 88-inch spiral-ridge cyclotron. After magnetic analysis, the beam had an energy resolution of 0.14% and was focused on a target at the center of the scattering chamber, a typical beam spot being 2 mm high by 1.5 mm wide. The exact angle at which the beam intersected the target was determined by observing via remote television two luminous foils, one at the target position, and the other 70 cm downstream. The beam current chosen for these experiments ranged from 60 to 800 nA depending upon experimental conditions, and was monitored by a Faraday cup connected to an integrating electrometer. The energy of the beam was inferred from measuring its range in aluminum.

Reaction products were detected in two independent counter telescopes located on opposite sides of the scattering chamber. Each consisted of a 150μ phosphorus-diffused silicon ΔE transmission counter operated in coincidence with a 3.0 mm lithium-drift silicon E counter; an additional 500μ lithium-drift silicon E-reject counter was operated in anticoincidence with the first two, thus eliminating long-range protons and deuterons. A single 1 mm monitor counter was fixed at $\theta_{lab} = 27.5°$ to observe any target deterioration or beam-energy changes during a series of measurements on a particular target.

For solid targets, a tantalum collimator 5 mm high by 2 mm wide was mounted 48 cm from the target, resulting in an angular resolution of 0.26° and an acceptance angle of 5×10^{-5} sr. Target gases were contained in a cell consisting of a cylindrical frame surrounded by a 315° continuous

window of 2.5μ Havar foil; the total enclosed volume was 47 cm^3. In order to define the gas target and to eliminate particles scattered from the gas cell window, a second collimator with the same width as the first was mounted 36 cm ahead of it.

A schematic diagram of the electronics is shown in Fig. 1. The energy signals from the counters in each system, preamplified in the experimental area, were transmitted to the counting area where, after further amplification and satisfaction of slow coincidence ($2\tau \approx 2\mu sec$) requirements, they were fed to a Goulding-Landis particle identifier. An output signal characteristic of the particle type was produced, and by means of a four-channel router this signal was subsequently used to route the total-energy signal into 1024 channel groups of a 4096-channel analyzer. The spectra recorded for each telescope corresponded to α-particles, ^{3}He-particles, tritons, and those particles slightly less ionizing than the selected triton group. The first and last groups were taken primarily to check that no ^{3}He particle or triton counts were lost. The relative efficiencies of the two systems was checked in several runs where the telescopes were placed at the same angle but on opposite sides of the beam. The result obtained was 1.00 ± 0.05.

The overall energy resolution (FWHM) observed throughout was 100-130 keV for tritons and 120-150 keV for ^{3}He-particles depending upon the target used.

III. EXPERIMENTAL RESULTS

If a target nucleus has isospin T_i, then the ratio of the differential cross-sections for (p,t) and (p,^{3}He) reactions leading to analogue final states with isospin $T_f = T_i + 1$ can be expressed simply when charge-dependent effects are neglected:

$$\frac{d\sigma/d\Omega(p,t)}{d\sigma/d\Omega(p,{}^3\mathrm{He})} = \frac{k_t}{k_{{}^3\mathrm{He}}} \times \frac{2\langle (T_i+1)(T_{z_i}+1)1\ 1 | T_i T_{z_i} \rangle^2}{\langle (T_i+1) T_{z_i}\ 1\,0 | T_i T_{z_i} \rangle^2} \quad . \tag{1}$$

Here k is the wave number of the outgoing particle and $\langle | \rangle$ is a Clebsch-Gordan coefficient. Thus, in this approximation, the differential cross-sections to analogue states should be identical in shape, and their magnitudes should be in the ratio $(k_t/k_{{}^3\mathrm{He}})$ when $T_f = 3/2$ and $(2k_t/3k_{{}^3\mathrm{He}})$ when $T_f = 2$. These properties provide an unambiguous experimental method for identifying analogue states.[11]

The analogue states having been identified, their excitation energies were determined by analyzing the data with the computer program LORNA.[12] This program establishes an energy scale by finding a least-squares fit to peaks whose Q-values are known, after correcting all incoming and outgoing particles for kinematic effects and absorber losses. For the data described here, contaminants were present or introduced in the targets, and well-known states produced from these contaminants were used in the calibrations. In particular, states produced from the reactions $^{12}C(p,t)^{10}C$ and $^{12}C(p,{}^3He)^{10}B$ were most useful throughout: the masses of the ground and first excited state of ^{10}C were taken from a recent re-evaluation by Brunnader et al.[13] while

information on the levels of ^{10}B was taken from Ajzenberg-Selove and Lauritzen.[14]

(A) $^{26}Mg(p,t)^{24}Mg$ and $^{26}Mg(p,^{3}He)^{24}Na$; T = 2 states: Figure 2 shows triton and ^{3}He spectra observed from a 1.26 mg/cm^2 self-supporting magnesium foil enriched to 99.2% in ^{26}Mg; the data were taken at $\theta_{lab} = 22.3°$ for 3200 μc. It is evident from the figure that a significant amount of carbon was present in the target, and the peaks corresponding to states in ^{10}C and ^{10}B provided the principal sources of calibration although all other peaks with (unbracketed) energies marked in the figure were also used.

The T = 2 states in ^{24}Mg and ^{24}Na have both been identified previously[15-19] and, in fact, the angular distribution of the (p,t) reaction to the state in ^{24}Mg has also been extensively studied.[20] Consequently, no attempt was made here to obtain angular distributions; both telescopes were set at $\theta_{lab} = 22.3°$, this being near a maximum in the L = 0 angular distribution as well as being an angle at which the analogue states were resolved from nearby impurity levels. Values for the excitation energies were obtained and the results are given in Table 1.[15-19,21-25] Also given in the table are weighted averages of all previous measurements, and a final overall average which also includes the present results.

Clearly, the precision of previous measurements[15-17] of the T = 2 state in ^{24}Mg precludes any improvement by our value, but the excellent agreement between the two may be taken as a measure of the reliability of our methods.

(B) $^{25}Mg(p,t)^{23}Mg$ and $^{25}Mg(p,^{3}He)^{23}Na$; $T = 3/2$ states: The spectra of tritons and ^{3}He observed from a 500μgm/cm^2 ^{25}Mg-enriched magnesium target are shown in Fig. 3. The components of the target were ^{24}Mg (8.29%), ^{25}Mg (91.54%), ^{26}Mg (0.17%) and, in addition, oxygen and carbon impurities. Spectra were obtained at six angles between $\theta_{lab} = 17.2°$ and $\theta_{lab} = 31.5°$, with the data in the figure being collected for 970 micro-Coulombs at $\theta_{lab} = 24.1°$.

Rough Coulomb-energy calculations indicate that the $T = 3/2$ analogue states should be at an excitation of about 7.8 MeV in ^{23}Mg and ^{23}Na. The peaks marked $T = 3/2$ in Fig. 3 are consistent with these expectations, and at the top of Fig. 4 is shown the angular distribution of corresponding tritons and ^{3}He particles, the experimental ^{3}He points having been multiplied by $k_t/k_{^3He}$ (= 0.92) in order to facilitate the comparison suggested by Eq. (1). The shapes and magnitudes of the distributions are the same within the expected accuracy of the approximations used in the derivation of Eq. (1) and thus, the $T = 3/2$ character of the levels is established. Also shown at the bottom of Fig. 4 are the angular distributions for the (p,t) reaction to the g.s. (3/2+) and 0.451 MeV state (5/2+) of ^{23}Mg. Since the spin-parity of ^{25}Mg is 5/2+, the former transition should be characterized predominantly by $L = 2$ transfer while the latter should have $L = 0$. By a simple comparison, the angular momentum transfer to the analogue states is determined to be predominantly $L = 0$. To provide added confirmation, distorted-wave Born approximation (DWBA) calculations were performed using a modified version of the computer program DWUCK[26] and the optical-model potentials listed in Table 2.[20] The results of computations which assumed

pure $L = 0$ or $L = 2$ transfer are shown normalized to the experimental points in Fig. 4. Evidently, the spin-parity of the $T = 3/2$ states is $5/2+$, indicating that they are analogues to the ground state of ^{23}Ne.

The energies of the analogue states were determined precisely by using as known the peaks whose energies are marked in Fig. 3; the principal calibration points in the (p,t) spectrum were the ground states of ^{10}C, ^{22}Mg, and ^{14}O while in the (p,^{3}He) spectrum they were the ground state of ^{10}B and the 2.31 MeV state ($T = 1$) in ^{14}N. The results are given in Table 1 where, for the case of the $T = 3/2$ level in ^{23}Na, it can be seen that there is good agreement with earlier measurements.[21,22] There has been no previous observation reported of the analogue state in ^{23}Mg.

(C) ^{22}Ne(p,t)^{20}Ne and ^{22}Ne(p,^{3}He)^{20}F; $T = 2$ states: In order to provide internal calibration points in the region of the $T = 2$ analogue states in mass-20, a mixture of 50% neon and 50% methane was used. The neon gas was 92.0% enriched in ^{22}Ne, the proportions of the remaining isotopes being 7.6% ^{20}Ne and 0.4% ^{21}Ne.

As was the case with the $T = 2$ states in mass-24, the lowest analogue states in ^{20}Ne and ^{20}F have been identified previously,[16,23-25] so no angular distributions were obtained in this experiment. Figure 5 shows triton and ^{3}He spectra taken at $\theta_{lab} = 36.2°$ for 9280 μc. Although the cross section for $L = 0$ transfer is relatively low at this angle, it is greater than for any other angle at which both $T = 2$ states are simultaneously resolved. The energies of the analogue states were again determined principally using states in ^{10}C and ^{10}B for calibration. The result for ^{20}Ne appears directly in Table 1 and agrees well with previous measurements. Additional data

IV. COULOMB DISPLACEMENT ENERGIES-CALCULATIONS

The potential which describes the Coulomb interaction between nucleons can be written as the sum of three operators, respectively having the properties of a scalar, a vector and a tensor in isospin space.[10,35] A general expression for the Coulomb energy of a nuclear state which involves A nucleons can be derived from this interaction using first-order perturbation theory. The result for a state with total isospin T and $T_z = \frac{N-Z}{2}$ is

$$E_c(A,T,T_z) = E^{(0)}(A,T) - T_z E^{(1)}(A,T) + [3T_z^2 - T(T+1)]E^{(2)}(A,T) \quad . \qquad (2)$$

The isoscalar, isovector and isotensor coefficients $E^{(0)}$, $E^{(1)}$ and $E^{(2)}$ depend only upon A, T and the details of the space-spin structure of the nuclear wave functions. They can be directly related to the coefficients in the isobaric multiplet mass equation (IMME):[36]

$$M(A,T,T_z) = a(A,T) + b(A,T)T_z + c(A,T)T_z^2 \quad . \qquad (3)$$

The IMME has been used successfully to describe the energies of states within isobaric multiplets with $T > 1$ and, with the possible exception of mass-9, no deviations from its predictions have been detected experimentally.[1] This result implies that for the cases under consideration a second or higher order perturbation treatment of the Coulomb interaction is not necessary or alternately that the effect of such a treatment is mostly absorbed by the coefficients of the quadratic equation.[2] In addition to the Coulomb interaction

other small charge-dependent effects such as the charge-dependent nuclear interaction and the electromagnetic spin-orbit interaction can also be treated as simple perturbations without affecting the form of the quadratic IMME. This means that an experimental determination of the coefficients in the IMME will include not only the effects of the Coulomb interaction but also other small charge-dependent effects. Ultimately, a comparison with calculations which include only Coulomb effects should yield a magnitude for any additional charge dependence. Such calculations, however, must be based on realistic nuclear wave functions using proper radii and they must, if necessary, include the corrections from a higher order perturbation treatment.

The purpose of the present investigation is to compare the experimental and calculated Coulomb displacement energies in the $(1d_{5/2})$-shell. In terms of those quantities defined in Eq. (2) the Coulomb displacement energy between neighboring isobars is given by

$$\Delta E_c(A,T,T_z-1|T_z) \equiv E_c(A,T,T_z-1) - E_c(A,T,T_z)$$
$$= E_c^{(1)}(A,T) - 3(2T_z-1)E^{(2)}(A,T) \quad . \qquad (4a)$$

The corresponding experimental quantity is

$$M(A,T,T_z-1) - M(A,T,T_z) + \Delta m \qquad (4b)$$

where Δm is the neutron-hydrogen mass difference (= 0.7824 MeV). Any discrepancy between calculations using Eq. (4a) and the experimental quantities (4b) may be interpreted as arising from one or several of the following factors: (i) the approximate nature of the nuclear wave functions used in the calculations; (ii) mathematical approximations introduced into the calculations for example by neglecting small terms; (iii) the presence of isospin mixing which means that the (2T+1) members of a multiplet are not simply related by the isospin ladder operators $T_{\pm}$, and indicates that the first order perturbation treatment used to derive Eq. (2) is no longer sufficient; and (iv) the presence of charge-dependent forces other than Coulomb forces.

Our approach will entail parameterizing Eq. (4a) according to calculations based on simple shell-model states and two different coupling schemes. The parameters will then be determined from a fit to data throughout the $(1d_{5/2})$-shell, and only the final parameter-values will be used for comparison.

(A) Low-seniority limit of the j-j coupling scheme: Theoretical expressions for $E^{(1)}$ and $E^{(2)}$ have been derived by Hecht[9] for shell-model states having the configuration j^n and seniority $v \leq 2$, the representation being chosen such that each state is defined by the four quantum numbers v, t (reduced isospin), J and T. These expressions are given in terms of two-body Coulomb-energy matrix-elements

$$V_{J'} = \left\langle j^2 J' \left| \frac{e^2}{3r_{ij}} \right| j^2 J' \right\rangle \qquad (5)$$

and the interaction of the protons in the j-shell with those in the core:

$$a_c = \sum_{J',j_c} \frac{(2J'+1)}{(2j+1)} \left\langle (jj_c)J' \left| \frac{e^2}{3r_{ij}} \right| (jj_c)J' \right\rangle . \quad (6)$$

In his formulation, there are three quantities which must be evaluated, or treated as free parameters; they are a_c, V_o and $\overline{V}_2$, where $\overline{V}_2$ is the average seniority-2 matrix element, i.e.:

$$\overline{V}_2 = \frac{1}{(2j-1)(j+1)} \sum_{\substack{J' \text{even} \\ >0}} (2J'+1)V_{J'} . \quad (7)$$

As detailed below, we have generalized Hecht's expressions in the manner described by Jänecke[3] so as to take account of additional non-Coulomb charge-dependent effects and the variation of the nuclear radius with mass number. This results in an increase in the number of free parameters to five. A direct comparison with experiment should become possible, and a subsequent analysis of the parameters obtained from the fit to a large quantity of experimental data should yield information on the two-body Coulomb-energy matrix elements as well as on the problems discussed previously.

To illustrate the method used, we shall consider an isobaric multiplet with configuration j^n and seniority 0. Expressions for $E^{(1)}$ and $E^{(2)}$ may be obtained from Table 1 of Reference 10:[37]

$$E^{(1)} = 3a_c + 3b(n-1) + 12c(j+1) \tag{8a}$$

$$E^{(2)} = b + c - c \frac{[(n-2j-1)^2 - (2j+4)^2]}{(2T-1)(2T+3)} \tag{8b}$$

where a_c has been defined in Eq. (6) and

$$b = \frac{2(j+1)\overline{V}_2 - V_o}{2(2j+1)} \tag{9}$$

$$c = \frac{V_o - \overline{V}_2}{4(2j+1)} \quad .$$

A formula for the Coulomb displacement energy could now be derived using Eq. (4a) and it would depend upon the three parameters a_c, b and c (or, equivalently, a_c, V_o and $\overline{V}_2$). However, additional charge-dependence will be expected to have the greatest effect upon the quantity c. In particular the electromagnetic spin-orbit interaction[38] between nucleons is expected to cause an increase in this parameter of as much as 40%. Furthermore, its increase in the tensor coefficient should be greater than in the vector coefficient by a factor ~ 1.7 (= $(g_p - g_n)/g_p$). Consequently, we replace the quantity c in Eq. (8a) by $c^{(1)}$ and in (8b) by $c^{(2)}$. It is important to note that $c^{(1)}$ and $c^{(2)}$ will in addition contain the effects of charge dependence in the nuclear force, but since these quantities are relatively

small, any inadequacy in the assumed wave functions or any approximation introduced into the calculation might also be expected to affect the values of $c^{(1)}$ and $c^{(2)}$ determined from experimental data.

One final consideration is the variation of the charge-radius with mass number, since this affects the values of the matrix elements in Eqs. (5) and (6). The Coulomb interaction radius R which is defined for any pair of protons will be assumed to vary according to

$$R \equiv \langle (j_1 j_2) J' | r_{ij}^{-1} | (j_1 j_2) J' \rangle^{-1} = R_o [1 + \lambda/3 \, \frac{n}{N}] \equiv R_o f(\lambda) \qquad (10)$$

where n is the number of active nucleons, N is the number of nucleons in the core, and R_o is a constant. The quantities R and R_o depend upon the values of j, j_c (if a core proton is involved) and J'; the function $f(\lambda)$ is assumed to be the same for all proton pairs. Equation (10) may be considered as the first term of a binomial expansion and, for $\lambda = 1$, would correspond approximately to an $A^{1/3}$ dependence of R. In the $(1d_{5/2})$-shell Eq. (10) becomes:

$$R = R_o [1 + \frac{1}{3} \lambda \, \frac{(A-16)}{16}] \ .$$

We have treated λ as a free parameter.

Having made these modifications to Eqs. (8), one may use Eq. (4a) to obtain a final expression for the Coulomb displacement energy which has the form

$$\Delta E_c(A,T,T_z-1|T_z) = [\alpha + \beta\ (\tfrac{n}{2} - T_z) + A_1\gamma^{(1)} + A_2\gamma^{(2)}][f(\lambda)]^{-1} \quad (11)$$

where

$$\alpha = 3a_c + 12c^{(1)}(j+1)$$

$$\beta = 6b$$

and $\gamma^{(i)} = 3c^{(i)}$ $\quad i = 1, 2$.

For the particular example chosen $(v = 0)$ the coefficient $A_1 = 0$ and A_2 is given by the formula quoted in the top line of Table 4. Also quoted in the same table are general formulae[39] for j^n configurations with $v = 1$ and $v = 2$; they were all calculated using expressions for $E^{(1)}$ and $E^{(2)}$ given in Table 1 of Reference 10. The expressions for the $v = 2$ cases had already been simplified by making use of the fact that, to a good approximation,[3] $V_{J'} = \overline{V}_2$ for all $J'(\text{even}) \geq 2$.

(B) Wigner supermultiplet scheme: Hecht[10] has derived general algebraic formulae for $E^{(1)}$ and $E^{(2)}$ assuming certain configurations in the Wigner supermultiplet scheme.[40] The supermultiplet quantum numbers, the total spin S and the isospin T were assumed to be good quantum numbers. Thus, the states are identified by L, S, T and $[\tilde{f}]$ where $[\tilde{f}]$ is the partition which characterizes a particular irreducible representation[41,42] of U_4. The form of $[\tilde{f}]$ is given by

$$[\tilde{f}] \equiv [x_1, x_2, x_3, x_4]$$

where $\sum_{i=1}^{4} x_i = n$ is the number of nucleons in the major oscillator shell, and $x_i \geq x_k$ when $i < k$. The Coulomb energies were assumed to be independent of the spatial quantum numbers. This should be a good approximation, but the expressions are even exact if applied to the average Coulomb energies for all states of an SU_6 multiplet in the (1d 2s)-shell.

The supermultiplet quantum numbers of the ground states have been predicted by Jahn[41] for nuclei throughout the d-shell. From these predictions certain patterns are apparent, and by using the formulae in Reference 10 we have derived general expressions for Coulomb displacement energies which apply to most ground-state supermultiplets throughout the shell. A single example will illustrate the method: consider those states for which $(\frac{n}{2} - T)$ and A are both even, i.e. analogues to the ground states of even-even nuclei. In addition to the fact that they must be $^1S_0$, Table 2 of Reference 41 indicates that all such states in the d-shell are characterized by partitions of the type [x+y, x+y, x, x]; for example, the d^6 state with $T = 1$ is [42] ≡ [2211]. In Table 1 of Reference 10 expressions for $E^{(1)}$ and $E^{(2)}$ are given for partitions of this type, and we have obtained a general equation for the Coulomb displacement energy in the manner already described for the seniority scheme. The result has the same form as Eq. (11), viz:

$$\Delta E_c\,(A,T,T_z-1|T_z) = [\alpha + \beta\,(\tfrac{n}{2} - T_z) + A_1\gamma^{(1)} + A_2\gamma^{(2)}][f(\lambda)]^{-1} \qquad (12)$$

but in this case: $\alpha = 3a_c' + 18c^{(1)'}$

$\beta = 6b'$

$\gamma^{(i)} = 3c^{(i)'} \quad i = 1, 2$.

Note that a_c', b' and $c^{(i)'}$ are primed, and appear in the notation of Reference 10. They can be expressed in terms of the two-body Coulomb-energy matrix elements which are the orbital angular momentum analogues of the corresponding matrix elements in the seniority scheme. For the example being discussed; $A_1 = 0$ and A_2 is given in the top line of Table 5.

General formulae for other ground-state configurations are also shown in Table 5. The only cases for which the existing formulae are insufficient are those multiplets based on the ground states of odd-odd nuclei with $T > 1$. A comparison of the formulae listed in Table 5 with those listed in Table 4 shows a number of striking similarities in spite of the dissimilarity of the coupling schemes used in their calculation, and suggests that they might also be expected to apply in some more realistic intermediate scheme.

V. COULOMB DISPLACEMENT ENERGIES - COMPARISON WITH EXPERIMENT

A complete summary of experimentally-determined Coulomb displacement energies throughout the $(1d_{5/2})$-shell, including those derived from the data in Table 1, is given in the fifth column of Table 6. The numbers quoted are weighted averages of data from the references given, and are intended to be complete up to September 1968. The table includes only those states for which, in the simplest model, all active nucleons can be considered to be in the $(1d_{5/2})$ shell. In addition, for each value of A and T, only multiplets built on ground states are considered, except for those $T = 1/2$ odd-A nuclei whose ground-state spins are not 5/2+; in these cases, the lowest excited 5/2+ states were used. The $T = 3/2$ multiplet with $A = 19$ is the only one for which the 5/2+ states are not known in all nuclei, and consequently the 3/2+ states were used. In all subsequent fitting, these two $T = 3/2$ mass-19 displacement energies were both included and removed; at no time was the overall fit changed in any way by their inclusion. The last two items in the table are double Coulomb displacement energies which are symbolized, in an obvious notation, by $\Delta E_c(A,T,T_z-2|T_z)$; their purpose will become apparent.

In Eq. (11), for the seniority scheme, and Eq. (12), for the supermultiplet scheme, the Coulomb displacement energy was given in terms of five parameters α, β, $\gamma^{(1)}$, $\gamma^{(2)}$ and λ. These equations have been fitted to the results in Table 6 by treating all five parameters as free, and then minimizing the function χ^2, where χ^2 is defined by

$$\chi^2 = \sum_{i=1}^{M} \left\{ \frac{\Delta E_c(\text{calc})i - \Delta E_c(\text{exp})i}{\sigma(\text{exp})i} \right\}^2 \qquad (13)$$

M is the total number of experimental values used in the fit, and $\sigma(\text{exp})$ is their experimental error. If the averaged experimental errors, as quoted in Table 6, represent a good approximation to the true standard deviation, then the chi-square test can be applied to the final χ^2_{min} obtained by minimizing Eq. (13). If all single displacement energies in Table 6 are used, M = 28, and the number of degrees of freedom of the assumed chi-square distribution is (28-5-1) = 22. Under these conditions, for an acceptable fit, χ^2_{min} should lie between 11 and 37. Since the method of determining experimental errors on energy measurements is at best inconsistent between different authors, and at worst totally arbitrary, it seems unlikely that such errors are any more than merely indicative of the true standard deviations. Consequently, the chi-square test should in this case be interpreted somewhat loosely.

The variation of χ^2 as a function of λ is shown in Fig. 9 for three cases in both the seniority and supermultiplet schemes. Each point on the graph corresponds to the result of minimizing χ^2 as a function of α, β, $\gamma^{(1)}$ and $\gamma^{(2)}$ for a particular choice of λ. The three cases considered are:

I. For the seniority scheme all the single displacement energies listed in Table 6 were used. For the supermultiplet scheme all single displacement energies were used with the exception of the T = 1 multiplets for A = 20 and 24. As indicated by the fourth line of Table 5,

such multiplets can have either $S = 0$ or 1, and the calculated displacement energies depend upon this choice. However, it is easy to show that when $T_z = +1$, the double Coulomb displacement energy is independent of S, and consequently the four single displacement energies involved were replaced by the two double values appearing at the end of the table.

II. The same values were used as in Case I except the two energies for ($T = 1$, $A = 18$) were removed.

III. The same values were used as in Case II except the single energy for ($T = 1/2$, $A = 19$) was also removed.

It is evident from the figure that both Case I and Case II result in totally unacceptable fits, as evidenced by the values of χ^2_{min}. For Case III, the seniority and supermultiplet calculations involve, respectively, 19 and 17 degrees of freedom for which the strict range of acceptable χ^2_{min} is 8 to 34 and 7 to 31. Considering the reservations stated previously, Case III must be deemed an acceptable fit. The values of the parameters λ, α, β, $\gamma^{(1)}$ and $\gamma^{(2)}$ for the minimum χ^2 for both calculations are shown in Table 7 in the columns headed "experimental", and the displacement energies calculated using these parameters are listed in columns 6 and 8 of Table 6. It can be seen that there is excellent agreement between the calculated displacement energies and also between the calculated and the experimental values. Finally, we should remark that the removal of other experimental energies from the fitting procedure does not result in any dramatic changes in either χ^2_{min} or the parameter values; in particular, the agreement between the values of λ obtained from both calculations remains good.

The anomalous behavior of the triplet with A = 18 presents an intriguing analogy with the case of mass 42 (see, for example, Refs. 2 and 3), both multiplets corresponding to n = 2 in their respective shells ($1d_{5/2}$ and $1f_{7/2}$). The behavior of both could be explained as being due to isospin mixing, but it is then unclear why only these multiplets are affected. An alternative hypothesis offered by Nolan et al.[4] to explain the mass-42 data was that the states involved have an anomalously large deformation. Using the values for the parameters α, β, $\gamma^{(1)}$ and $\gamma^{(2)}$ listed in Table 7, we again fitted the mass-18 data by varying λ; although it was indeed possible to reproduce the ^{18}O - $^{18}F^*$ energy difference by increasing the interaction radius $\sim$ 1% from its "average" value, the $^{18}F^*$ - ^{18}Ne mass difference indicated a reduction in the radius by $\sim$ 1%. Such inconsistency makes deformation appear to be an improbable explanation.

The mass-18 and mass-42 triplets were also investigated recently by Bertsch.[44] He considered additional correlations between proton pairs generated by excitations into higher shells. These correlations should affect the interaction between the two protons outside the core in the nuclei ^{18}Ne and ^{42}Ti. The experimental evidence, however, seems to indicate that the anomalous behavior of the triplets involves mostly the T = 1 states in ^{18}F and ^{42}Sc, respectively. In addition it is not clear why such correlations should affect only nuclei with n = 2. As a refinement to the above effect

one may have to consider a change in the interaction with the core. In conclusion, the relationship between the findings of Bertsch and the present analysis is not entirely clear.

Still another possibility for explaining the mass-18 anomaly is suggested by the relatively poor agreement for the A = 19 doublet. Here, although isospin mixing is unlikely, the wave function is certainly complex as evidenced by the fact that the lowest 5/2+ state in ^{19}F is its second excited state. Calculated wave functions[43] for this state indicate that the $[111]^{22}D$ component comprises only 50% of the total wave function as compared to an assumed 100% for the supermultiplet scheme; in addition, there are significant (2s)-shell admixtures. Equivalently, in j-j coupling, the $(d_{5/2})^3$ component is only 39% of the total strength. Although the similarity of Eqs. (11) and (12) has been used to predict a more general applicability, their accuracy under these conditions is uncertain, particularly considering that there are admixtures from another subshell. Since such admixtures appear to be appreciable only at the beginning of the $(1d_{5/2})$-shell, it is possible that they are the cause of our failure to fit the mass-18 and -19 data. However, final verification must certainly await more detailed calculations.

Also shown in Table 7 are values of V_o and $\overline{V}_2$ obtained from the "best fit" parameters in both schemes; these are compared with calculations using harmonic oscillator wave functions.

Table 7 shows in the columns denoted by "experimental" the parameters λ, α, β, $\gamma^{(1)}$ and $\gamma^{(2)}$ which were obtained from the least-squares analysis of the experimental Coulomb displacement energies in terms of Eqs. (11) or (12). The columns contain in addition the quantities a_c, b, etc.

which were calculated from α, β, etc. . The quantities γ and c cannot be derived directly from the experimental data, and certain assumptions have to be made as will be outlined subsequently. The two-body Coulomb-energy matrix-elements V_o, and $\bar{V}_2$, finally were obtained in the seniority scheme with the use of Eq. (9). Because of the n-dependence of the Coulomb interaction radii defined by Eq. (10), the two-body matrix-elements decrease with increasing A. The pairs of values for V_o, and $\bar{V}_2$, shown refer to the beginning and the end of the $(1d_{5/2})$-shell, respectively.

Also shown in Table 7 are values for the various coefficients and matrix-elements which were calculated[45] using harmonic oscillator wave functions. A value of $\hbar w = [41/(22)^{1/3}]$ MeV was used to obtain the oscillator constant $e^2\sqrt{(m\omega)/(2\pi\hbar)}$. Electromagnetic spin-orbit effects were included[38] in the calculations of $c^{(1)}$ and $c^{(2)}$ in the seniority scheme. The theoretical ratio $c/(c^{(1)} + c^{(2)})$ was used to estimate c(exp) from $c^{(1)}$(exp) and $c^{(2)}$(exp). This procedure is not very accurate, and the values of c(exp) are given with rather large estimated uncertainties. As a consequence, the experimental matrix-element V_o has also a rather large uncertainty.

There is good agreement between the experimental and calculated coefficients b both in the seniority and supermultiplet scheme. Further, the experimental coefficient a_c agrees well between the two schemes. The small coefficients c, however, do not agree very well. The experimental values exceed the calculated ones by factors of about 1.4 in the seniority scheme,

and about 3.9 in the supermultiplet scheme. This result seems to indicate that the Coulomb pairing energy is larger than predicted by the calculations, particularly in the supermultiplet scheme. The latter result is probably due to the approximations introduced into the derivation of the supermultiplet equations. It is concluded that pairing in the ground and low excited states is about 4 times stronger than for the average of the states belonging to the same supermultiplet.

The quantities $c^{(1)}$ and $c^{(2)}$ do not show the expected behavior. The ratio $c^{(2)}/c^{(1)}$ should be greater than one because of the contributions from the electromagnetic spin-orbit interaction. Contributions from charge-symmetric charge-dependent nuclear forces, should further increase this ratio. The experimental ratio $c^{(2)}/c^{(1)}$ obtained in the seniority scheme is less than one, and in the supermultiplet scheme the individual values are already much too big. The somewhat irregular behavior of these quantities, is probably the result of the underlying simplifying assumptions for the theoretical equations. In addition to contributions from the electromagnetic spin-orbit interaction and the charge-dependent nuclear interaction, the small experimental quantities $c^{(1)}$ and $c^{(2)}$, when treated as adjustable parameters, have to absorb the approximations introduced into the supermultiplet equations, possible contributions from isospin mixing (second order perturbations), and the inadequacies of the assumed configurations and coupling schemes.

The experimental two-body Coulomb-energy matrix-elements V_o and $\overline{V}_2$ which were obtained with the use of the seniority equations can be compared

to two sets of calculated values. One set was calculated[45] using harmonic oscillator wave functions as described above. The other set (in square brackets) was calculated[44] by considering additional correlations between proton pairs generated by excitations into higher shells. The experimental values lie in between the two calculated values which seems to indicate that such correlations may be present. However, a similar comparison[3] for the $(1f_{7/2})$-shell showed no enhancement of the experimental values. It should also be noted that the use of more realistic wave functions such as those which are generated by a reasonable Woods-Saxon well will undoubtedly change the calculated matrix-elements to a certain extent.

VI. MASS PREDICTIONS

Using the parameters listed in Table 7 it is, of course, possible to calculate any Coulomb displacement energy within the $(1d_{5/2})$-shell. Thus, if the mass of any member of a multiplet is known, the masses of all other members can be readily predicted. We have calculated in this manner the masses, as yet unmeasured, of six neutron-deficient nuclei. The results for both schemes are shown in Table 8 [46] where the quoted errors only include the experimental error in the masses upon which the predictions depend. For example, the mass of ^{25}Si is derived by adding the displacement energy minus the neutron-hydrogen mass difference (0.7824 MeV) to the mass of the $T = 3/2$ analogue state in ^{25}Al; since the experimental error on the energy of that state is ±8 keV, that is the error quoted in Table 8. The agreement between calculations with the two coupling schemes is extremely good with the possible exception of ^{24}Si and even for it the discrepancy is only 48 keV. Also shown in the table are the predictions of Kelson and Garvey; [46] they are consistently lower than ours but never by more than 125 keV.

Based on the predictions in Table 8, the undiscovered nuclei ^{20}Mg and ^{24}Si are certainly stable, since their last proton is bound by more than 2.70 MeV. The nuclei ^{22}Al and ^{23}Al are predicted stable against proton emission by 0.15 and 0.16 MeV respectively, while ^{19}Na is predicted unstable by 0.36 MeV.

In a similar manner, the excitation energies of $T = 2$ states in some $T_z = \pm 1$ and 0 nuclei have been calculated, and the results are tabulated in Table 9. [47] The mass-22 multiplet is assumed to have seniority 2, and consequently the relevant predictions depend upon whether the J of the state

is even or odd. Since the ^{22}F ground state is probably 1+,[47] the predictions for odd-J are more likely correct.

Finally, the mass difference for all remaining members of multiplets within the $(1d_{5/2})$ shell have been calculated and are tabulated in Table 10. It should be noted that we have tabulated mass differences, the neutron-hydrogen mass difference having been included. Thus, for example, if the mass of ^{21}O were known, the mass of its $T = 5/2$ analogue in ^{21}F could be calculated in the seniority scheme by adding 2.712 MeV.

VII. CONCLUSIONS

A detailed comparison between twenty-eight experimental Coulomb displacement energies in the $(1d_{5/2})$-shell and the values obtained with Hecht's Coulomb energy equations shows very good agreement. Two sets of equations were considered, the one being derived in the low-seniority j-j coupling limit, and the other in the Wigner supermultiplet scheme; the fact that both worked about equally well seems to indicate that Coulomb energies are relatively insensitive to the assumed coupling scheme. The agreement between the experimental and calculated displacement energies was obtained by treating five coefficients as adjustable parameters and subjecting the data to a least-squares analysis. One of the parameters is related to the Z- and N-dependence of the charge radius. It was found that the two-body Coulomb-energy matrix elements decrease by about 9% throughout the $(1d_{5/2})$-shell; the other parameters are directly related to these matrix-elements. Reasonable agreement exists between the experimental and calculated values where the latter were obtained by using harmonic oscillator wave functions. However, the experimental Coulomb pairing energy is somewhat greater than the calculated values. Information about the electromagnetic spin-orbit interaction and about the charge-dependent nuclear interaction cannot be extracted at present probably due to the simplifying assumptions underlying the derivation of the theoretical equations. The fact that the calculated displacement energies reproduced the experimental values so accurately did permit the masses of certain unknown proton-rich nuclei and excitation energies of unknown isobaric analogue states to be predicted with a high probable accuracy.

FOOTNOTES AND REFERENCES

*Work performed under the auspices of the U. S. Atomic Energy Commission.

1. J. Cerny, Annual Review of Nuclear Science 18, 27 (1968).
2. J. Jänecke, Bull. Am. Phys. Soc. 13, 1402 (1968).
3. J. Jänecke, Nucl. Phys. A114, 433 (1968).
4. J. A. Nolen, J. P. Schiffer, N. Williams, and D. van Ehrenstein, Phys. Rev. Letters 18, 1140 (1967).
5. M. Harchol, A. A. Jaffe, J. Mirion, I. Unna, and J. Zioni, Nucl. Phys. A90, 459 (1967).
6. R. Sherr, Phys. Letters 24B, 321 (1967).
7. B. C. Carson and I. Talmi, Phys. Rev. 96, 436 (1964).
8. A. de-Shalit and I. Talmi, Nuclear Shell Theory (Academic Press, New York, 1963).
9. K. T. Hecht, Nucl. Phys. A102, 11 (1967).
10. K. T. Hecht, Nucl. Phys. A114, 280 (1968); see also K. T. Hecht and S. C. Pang, to be published.
11. J. Cerny and R. H. Pehl, Phys. Rev. Letters 12, 619 (1964).
12. LORNA is a program written by C. C. Maples, whom we thank for making it available.
13. H. Brunnader, J. C. Hardy, and Joseph Cerny, Phys. Rev. 174, 1247 (1968).
14. F. Ajzenberg-Selove and T. Lauritzen, Nucl. Phys. A114, 1 (1968).
15. G. T. Garvey, J. Cerny, and R. H. Pehl, Phys. Rev. Letters 12, 726 (1964).
16. E. Adelberger and A. B. McDonald, Phys. Letters 24B, 270 (1967); and erratum, Phys. Letters 24B, 618 (1967).

17. F. Riess, W. J. O'Connell, D. W. Heikkinen, H. M. Kuan, and S. S. Hanna, Phys. Rev. Letters 19, 327 (1967).

18. G. T. Garvey and J. Cerny, unpublished.

19. F. G. Kingston, R. J. Griffiths, A. R. Johnston, W. R. Gibson, and E. A. McClatchie, Phys. Letters 22, 458 (1966).

20. S. W. Cosper, H. Brunnader, J. Cerny, and R. L. McGrath, Phys. Letters 25B, 324 (1967).

21. S. Mubarakmand and B. E. F. Macefield, Nucl. Phys. A98, 97 (1967), and private communication.

22. J. Dubois, Nucl. Phys. A104, 657 (1967).

23. J. Cerny, R. H. Pehl, and G. T. Garvey, Phys. Letters 12, 234 (1964).

24. H. M. Kuan, D. W. Heikkinen, K. A. Snover, F. Riess, and S. S. Hanna, Phys. Letters 25B, 217 (1967).

25. R. Bloch, R. E. Pixley, and P. Truöl, Phys. Letters 25B, 215 (1967).

26. The program DWUCK was written by D. Kuntz; we appreciate his making it available. The modification for two-nucleon transfer was made by us, and follows the "zero-range interaction" approximation.[27]

27. N. K. Glendenning, Phys. Rev. 137, B102 (1965).

28. R. D. Gill, B. C. Robertson, J. L'Ecuyer, R. A. I. Bell, and H. J. Rose, Phys. Letters 28B, 116 (1968).

29. E. Adelberger, Thesis, California Institute of Technology, unpublished.

30. J. H. Towle and G. J. Wall, Nucl. Phys. A118, 500 (1968).

31. Although this peak is not clearly resolved in Fig. 6 from the 1.74 MeV state in ^{10}B, it should be pointed out that this was not the case at the other angles observed.

32. Nolan F. Mangelson, B. G. Harvey, and N. K. Glendenning, Nucl. Phys. A117, 161 (1968).

33. There are no states in ^{19}Ne known to be 3/2+ and consequently there could be no "known" L = 0 angular distributions to states in that nucleus. Instead, for comparison, the L = 0 distribution of the ^{20}Ne(p,t)^{18}Ne g.s. was used in Fig. 8. It should be noted however, that the obvious L = 0 distribution to the 4.013 MeV state in ^{19}Ne identifies it, as well as the analogue state, to be 3/2+.

34. J. W. Butler, L. W. Fagg, and H. D. Holmgren, Phys. Rev. 113, 268 (1959).

35. J. Jänecke, Phys. Rev. 147, 735 (1966).

36. E. P. Wigner, Proc. Robert A. Welch Foundation Conference on Chemical Research, Ed. by W. O. Milligan, (The Robert A. Welch Foundation, Houston, 1958) p. 67; S. Weinberg and S. B. Treiman, Phys. Rev. 116, 465 (1959); D. H. Wilkinson, Isobaric Spin in Nuclear Physics, Ed. by J. D. Fox and D. Robson, (Academic Press, New York, 1966) p. 30.

37. These may be shown equivalent to the quantities appearing in Eqs. (86-90) of Ref. 9., by utilizing the relation

$$V_{even} = \frac{\overline{V}_o}{j(2j+1)} + \frac{\overline{V}_2(2j-1)(j+1)}{j(2j+1)} \quad .$$

38. K. T. Hecht, Isobaric Spin in Nuclear Physics, Ed. by J. D. Fox and D. Robson, (Academic Press, New York, 1966) p. 823.

39. It should be noted that the formulae for $v = 0$ and $v = 1$ are simply generalizations of Eqs. (6) and (7) of Ref. 2, where they were written exclusively for the 7/2-shell. Our definitions of α, b, and $\gamma^{(i)}$ are entirely equivalent.

40. E. Wigner, Phys. Rev. 51, 106 (1937).

41. H. A. Jahn, Proc. Roy. Soc. A201, 516 (1950).

42. H. A. Jahn and H. van Wieringen, Proc. Roy. Soc. A209, 502 (1951).

43. J. P. Elliot and B. H. Flowers, Proc. Roy. Soc. A229, 536 (1955).

44. G. F. Bertsch, Phys. Rev. 174, 1313 (1968).

45. K. T. Hecht, private communication.

46. I. Kelson and G. T. Garvey, Phys. Letters 23, 689 (1966).

47. R. H. Stokes and P. G. Young, to be published.

Table 1. Summary of experimental results.

Nucleus	Analogue State J^{π},T	Excitation Energy This work (MeV±keV)	Previous work (MeV±keV)	Ref.	Average value (MeV±keV)
^{24}Mg	$0^+,2$	15.426±30	15.436±5	15-17	15.436±5
^{24}Na	$0^+,2$	5.978±35	5.98±48	18,19	5.979±28
^{23}Mg	$5/2^+,3/2$	7.788±25	not reported	-	7.788±25
^{23}Na	$5/2^+,3/2$	7.910±30	7.890±30	21,22	7.900±21
^{20}Ne	$0^+,2$	16.722±25	16.732±2.4	16,23-25	16.732±2.4
^{20}F	$0^+,2$	6.523±35	6.43±100	23	6.513±33
^{19}Ne	$3/2^+,3/2$ [a]	7.620±25	not reported	-	7.620±25
^{19}F	$3/2^+,3/2$ [a]	7.660±35	not reported	-	7.660±35

[a] These levels are not the lowest-energy T = 3/2 levels in mass-19, but are analogues to the first excited state (0.095 MeV) of ^{19}O.

Table 2. Optical-model parameters[20] used in DWBA calculations.

Target	Projectile	V	W_s	r	a
^{20}Ne, ^{21}Ne	p	51.5	19.0	1.25	0.5
	t, ^{3}He	162.0	37.5	1.25	0.6
^{25}Mg	p	51.5	19.0	1.15	0.5
	t, ^{3}He	162.0	37.5	1.15	0.6

Table 3. Excited States of ^{18}Ne

This Work (MeV ± keV)	Previous Work (MeV ± keV)	Average (MeV ± keV)
g.s	g.s	-
1.890 ± 20	1.8873 ± 0.2[28]	1.8873 ± 0.2[a]
3.375 ± 30	3.3762 ± 0.4[28]	3.3762 ± 0.4
3.588 ± 25[a,b]	3.5763 ± 2.0[28]	3.5763 ± 2.0
	3.6164 ± 0.6[28]	3.6164 ± 0.6
4.580 ± 30	4.558 ± 13.5[29,30]	4.562 ± 12.2
5.115 ± 25	5.140 ± 18[29]	5.132 ± 15[a]

[a] These values were used as known in the analysis of $^{21}Ne(p,t)^{19}Ne$.

[b] This value was used in the analysis of $^{21}Ne(p,t)^{19}Ne$ because it represents the effective energy of the unresolved mixture of the (0^+) state at 3.5763-MeV, and the $2^{(+)}$ state at 3.6164-MeV, both populated by the (p,t) reaction.

Table 4. Coefficients in the expansion of the Coulomb displacement energy; $\Delta E_c(A,T,T_z-1|T_z) = [\alpha + (\frac{n}{2} - T_z)\beta + A_1\gamma^{(1)} + A_2\gamma^{(2)}][f(\lambda)]^{-1}$, where A_1 and A_2 are listed for configurations j^n in the seniority scheme.

v	t	J	A_1	A_2
0	0	0	0	$-(2T_z-1)\left[1+\frac{(2j+4)^2-(n-2j-1)^2}{(2T-1)(2T+3)}\right]$
1	1/2	j	$\frac{(n-2j-1)-(-)^{n/2-T}(2T+1)(2j+3)}{2T(T+1)}$	$-(2T_z-1)\left[1+\frac{(2j+3)^2-(n-2j-1)^2}{4T(T+1)}\right]$
2	0	odd	0	$-(2T_z-1)\left[1+\frac{(2j+2)^2-(n-2j-1)^2}{(2T-1)(2T+3)}\right]$
2	1	even,>0	$\frac{2(n-2j-1)}{T(T+1)}$	$-(2T_z-1)\left[1+\frac{(2j+1)(2j+3)-(n-2j-1)^2}{T(T+1)}\right.$ $\left.-\frac{3(2j+2)^2-3(n-2j-1)^2}{(2T-1)(2T+3)}\right]$

UCRL-18566

Table 5. Coefficients in the expansion of the Coulomb displacement energy, $\Delta E_c(A,T,T_z-1|T_z) = [\alpha + (\frac{n}{2} - T_z)\beta + A_1\gamma^{(1)} + A_2\gamma^{(2)}][f(\lambda)]^{-1}$ where A_1 and A_2 are listed for various ground state configurations in the d shell using the supermultiplet scheme. The Wigner supermultiplet quantum numbers are denoted by $[\tilde{f}]$.

$[\tilde{f}]$	S	J	$\frac{n}{2}-T$	x	A_1	A_2
$[x+y,x+y,x,x]^a$	0	0	even	$\frac{n-2T}{4}$	0	$-(2T_z-1)\left[\frac{6}{(2T-1)}\right]$
$[x+y,x+y,x+1,x]$	1/2	3/2,5/2	odd	$\frac{n-2T-2}{4}$	$-(-)^{\frac{n}{2}-T}\left[\frac{3}{T}\right]$	$-(2T_z-1)\left[\frac{3}{T}\right]$
$[x+y,x+y-1,x,x$	1/2	3/2,5/2	even	$\frac{n-2T}{4}$		
$[x+2,x+1,x+1,x]^b$	0,1	2,3,4	odd	$\frac{n-4}{4}$	0	$(2T_z-1)\left[6 - 4S(S+1)\right]$

a. $T > 0$

b. Only applies to ground states when $T = 1$

Table 6. Experimental and calculated Coulomb displacement energies.

A	T	T_z	J^π	Experimental $\Delta E_c(A,T,T_z-1\|T_z)$ (keV)	Seniority Calculations ΔE_c (keV)	Seniority Calculations ΔE_c(calc) $-\Delta E_c$(exp) (keV)	Supermultiplet Calculations ΔE_c (keV)	Supermultiplet Calculations ΔE_c(calc) $-\Delta E_c$(exp) (keV)
17	1/2	+1/2	5/2+	3542.0±1.0[a]	3542.2	0.2	3542.8	0.6
19	1/2	+1/2	5/2+*	4060.8±2.0[b,c]	4104.3	43.5†	4103.2	42.4†
21	1/2	+1/2	5/2+*	4315.3±8.3[b,d]	4316.6	1.3	4314.8	-0.5
23	1/2	+1/2	5/2+*	4850.5±4.7[b]	4861.1	10.6	4860.0	9.5
25	1/2	+1/2	5/2+	5062.5±1.1[e]	5062.6	0.1	5062.2	-0.3
27	1/2	+1/2	5/2+	5592.5±3.2[b]	5590.3	-2.2	5592.8	0.3
18	1	+1	0+	3478.9±1.0[a,f]	3549.4	70.5†	3510.4	31.5†
20	1	+1	2+	4027.8±8.4[b,g]	4024.9	-2.9	--	--
22	1	+1	0+	4282.1±2.8[b,h]	4279.0	-3.1	4280.0	-2.1
24	1	+1	4+	4783.5±4.6[b,i]	4790.2	6.7	--	--
26	1	+1	0+	5014.8±4.2[b]	5021.1	6.3	5025.0	10.2
18	1	0	0+	4187.6±4.8[a,f]	4142.8	-44.8†	4137.6	-50.0†
20	1	0	2+	4420.9±30.8[b,g]	4386.3	-34.6	--	--
22	1	0	0+	4931.6±20.2[b,h]	4901.2	-30.4	4897.0	-34.6
24	1	0	4+	5148.7±7.7[b,i]	5144.9	-3.8	--	--
26	1	0	0+	5623.2±11.6[b]	5592.8	-30.4	5632.1	8.9
19	3/2	+3/2	3/2+	3528.3±35.9[j,k]	3524.6	-3.7	3501.8	-26.5
21	3/2	+3/2	5/2+	3954.4±9.2[l]	3964.7	10.3	3944.9	-9.5
23	3/2	+3/2	5/2+	4302.7±21.3[j,m]	4268.8	-33.9	4268.4	-34.3
25	3/2	+3/2	5/2+	4743.4±15.8[n]	4707.1	-36.3	4698.2	-45.2

(continued)

Table 6. Continued.

A	T	T_z	J^π	Experimental $\Delta E_c(A,T,T_z-1\|T_z)$ (keV)	Seniority Calculations ΔE_c (keV)	Seniority Calculations ΔE_c(calc) $-\Delta E_c$(exp) (keV)	Supermultiplet Calculations ΔE_c (keV)	Supermultiplet Calculations ΔE_c(calc) $-\Delta E_c$(exp) (keV)
19	3/2	+1/2	3/2+	3980.4±43.0[j,k]	3997.3	16.9	3989.0	8.6
21	3/2	+1/2	5/2+	4440.4±9.2[l]	4439.6	-0.8	4428.1	-12.4
23	3/2	+1/2	5/2+	4726.0±32.7[j,m]	4739.3	13.3	4747.7	21.7
25	3/2	+1/2	5/2+	5161.4±15.3[n]	5166.7	5.3	5173.6	12.2
20	2	+2	0+	3484.4±33.9[a,j]	3516.0	31.6	3481.7	-2.7
24	2	+2	0+	4292.4±29.7[a,j,q]	4259.9	-33.1	4245.5	-46.9
20	2	+1	0+	3971.4±33.0[a,j,p]	3986.4	15.0	3966.8	-4.6
24	2	+1	0+	4724.4±28.4[r]	4721.0	-3.4	4722.8	-1.6
20	1	+1	2+	8448.7±31.9[‡,b]	--	--	8418.8	-29.9
24	1	+1	4+	9932.2±9.0[‡,b]	--	--	9923.0	-9.2

*These states are not ground states but the lowest excited 5/2+ states.

†These values were not used in the χ^2 fit.

‡These values are double Coulomb displacement energies.

[a] C. C. Maples, G. W. Goth, and J. Cerny, Nucl. Data A2, 429 (1966).

[b] P.M. Endt and C. Van der Leun, Nucl. Phys. A105, 1 (1967).

[c] F. Ajzenberg-Selove and T. Lauritzen, Nucl. Phys. 11, 1 (1959); J. W. Olness, A. R. Poletti and E. K. Warburton, Phys. Rev. 161, 1131 (1967).

[d] T. Lauritzen and F. Ajzenberg-Selove, Nucl. Data Sheets, May (1962).

(continued)

Table 6. Continued

[e] C. Van der Leun, private communication (1968) giving the mass excesses of ^{25}Al and ^{25}Mg as -8.9145±0.0021 MeV and -13.1947±0.0018 MeV, respectively.

[f] A. E. Blaugrund, D. H. Youngblood, G. C. Morrison, and R. E. Segel, to be published; E. K. Warburton, J. W. Olness, and A. R. Poletti, Phys. Rev. 155, 1164 (1967).

[g] R. D. MacFarlane and A. Siivola, Nucl. Phys. 59, 168 (1964); J. D. Pearson and R. H. Spear, Nucl. Phys. 54, 434 (1964).

[h] A. Gallman, G. Frick, E. K. Warburton, D. E. Alberger, and S. Hechtl, Phys. Rev. 163, 1190 (1967).

[i] A. J. Armini, J. W. Sunier, and J. R. Richardson, Phys. Rev. 165, 1194 (1967).

[j] This work.

[k] J. L. Wiza and R. Middleton, Phys. Rev. 143, 676 (1965); F. A. El Bedewi, M. A. Fawzi, and N. S. Rigk, Proc. Int'l. Conf. on Nucl. Phys. (Paris, 1964); R. Moreh and A. A. Jaffe, Proc. Phys. Soc. (London) 84, 330 (1964).

[l] H. Brunnader, J. C. Hardy, and J. Cerny, to be published; D. C. Hensley, Phys. Letters 27B, 644 (1968); A. B. McDonald and E. G. Adelberger, Phys. Letters 26B, 380 (1968).

[m] S. Mubarakmand and B. E. F. Macefield, Nucl. Phys. A98, 97 (1967) and private communication from B. E. F. Macefield; J. Dubois, Nucl. Phys. A104, 657 (1967).

[n] J. C. Hardy and D. J. Skyrme in Isotopic Spin in Nuclear Physics, Ed. by J. D. Fox and D. Robson, (Academic Press, New York, 1966) p. 701; D. Denhard and J. L. Yntema, Phys. Rev. 160, 964 (1967); G. C. Morrison, D. H. Youngblood, R. C. Bearse, and R. E. Segel, Suppl. J. Phys. Soc. Japan 24, 143 (1968). These values have been appropriately corrected for the changes noted in Ref. e.

(continued)

Table 6. Continued

[p] E. Adelberger and A. B. McDonald, Phys. Letters 24B, 270 (1967); H. M. Kuan, D. W. Heikkinen, K. A. Snover, F. Riess, and S. S. Hanna, Phys. Letters 25B, 217 (1967); R. Block, R. E. Pixley, and P. Truöl, Phys. Letters 25B, 215 (1967).

[q] F. G. Kingston, R. J. Griffiths, A. R. Johnston, W. R. Gibson, and E. A. McClatchie, Phys. Letters 22, 458 (1966).

[r] E. Adelberger and A. B. McDonald, Phys. Letters 24B, 270 (1967); F. Riess, W. J. O'Connell, D. W. Heikkinen, H. M. Kuan, and S. S. Hanna, Phys. Rev. Letters 19, 367 (1967).

Table 7. Experimental and calculated parameters for the $(1d_{5/2})$-shell. The experimental values result from a least-squares fit of the Coulomb displacement energies. The calculated values were obtained using a harmonic oscillator potential.

Quantity	Seniority Scheme		Supermultiplet scheme	
	Experimental[a]	Calculated[a]	Experimental[a]	Calculated[a]
λ	0.23±0.03		0.19±0.03	
α	3673±3		3643±3	
β	419±6	391.2	421±6	411.2
$\gamma^{(1)}$	8.14±0.09	4.80	14.40±0.12	
$\gamma^{(2)}$	6.41±0.03	5.28	1744±0.15	
γ	5.89±1.50	4.08	12.89±3.20	3.33
a_c	1186.3±1.2		1185.5±1.1	
b	69.8±1.0	65.2	70.2±1.0	68.5
$c^{(1)}$	2.71±0.03	1.60	4.80±0.04	
$c^{(2)}$	2.14±0.01	1.76	5.81±0.05	
c	1.96±0.50	1.36	4.29±1.10	1.11
V_o	(195/184)±14[b]	168[211][c]		
V_2		142[165][c]		
V_4		132[140][c]		
$\bar{V}_2$	(148/140)±3[b]	136[149][c]		

[a] All values, except λ, in keV.

[b] The two values shown refer to the beginning and the end of the shell respectively.

[c] The value shown in square brackets was calculated by considering additional correlations between proton pairs; see text.

Table 8. Mass predictions for neutron-deficient nuclei within the $(d_{5/2})$ shell.

Nucleus	Mass excess calculated using:		Garvey-Kelson prediction[46] (MeV)
	Seniority scheme (MeV±keV)[a]	Supermultiplet scheme (MeV±keV)[a]	
^{19}Na	12.965±25[b]	12.968±25[b]	12.87
^{20}Mg	17.509±2	17.510±2	17.40
^{21}Mg	10.916±7	10.910±7	10.79
^{22}Al	18.059±30	-	17.93[d]
^{23}Al	6.743±25	6.758±25	6.71
^{24}Si	10.765±5	10.813±5	10.72
^{25}Si[c]	3.828±8	3.804±8	3.77

[a]The errors quoted only include the experimental error in the masses upon which the predictions depend; see text.

[b]The ground state mass-excess is calculated assuming that the lowest 3/2+ state in ^{19}Na is at 0.095 MeV, as in its mirror ^{19}O.

[c]The decay but not the mass of this nucleus is known.

[d]This mass was recalculated using the new mass[47] for ^{22}F.

Table 9. Predicted excitations of unobserved T = 2 analogue states in $(1d_{5/2})$-shell nuclei.

Nucleus	J	Excitation energy of T = 2 state calculated using Seniority scheme (MeV±keV)[a]	Supermultiplet scheme (MeV±keV)[a]
^{20}Na	0+	6.492±30	6.486±30
^{22}Ne	even	14.011±30[b]	
	odd	13.987±30	
^{22}Na	even	14.760±30	
	odd	14.727±30	
^{22}Mg	even	13.978±35	
	odd	13.953±35	
^{24}Al	0+	5.954±9	5.971±9

[a]The errors quoted only include the experimental error in the masses upon which the predictions depend.

[b]All mass-22 predictions depend upon the mass excess of ^{22}F being 2.828± 0.030 MeV.[47]

Table 10. Predicted mass differences between different members of T = 5/2 and 3 isobaric multiplets in the $(1d_{5/2})$ shell.

T	Mass-difference between analogue states in:	Mass difference calculated with Seniority scheme (MeV)	Supermultiplet scheme (MeV)
5/2	$^{21}Al - ^{21}Mg^*$	4.492	4.508
5/2	$^{21}Mg^* - ^{21}Na^*$	4.047	4.054
5/2	$^{21}Na^* - ^{21}Ne^*$	3.602	3.600
5/2	$^{21}Ne^* - ^{21}F^*$	3.157	3.145
5/2	$^{21}F^* - ^{21}O$	2.712	2.691
5/2	$^{23}Si - ^{23}Al^*$	4.893	4.911
5/2	$^{23}Al^* - ^{23}Mg^*$	4.452	4.460
5/2	$^{23}Mg^* - ^{23}Na^*$	4.012	4.010
5/2	$^{23}Na^* - ^{23}Ne^*$	3.571	3.559
5/2	$^{23}Ne^* - ^{23}F$	3.130	3.108
3	$^{22}Si - ^{22}Al^*$	4.915	4.937
3	$^{22}Al^* - ^{22}Mg^*$	4.472	4.484
3	$^{22}Mg^* - ^{22}Na^*$	4.029	4.032
3	$^{22}Na^* - ^{22}Ne^*$	3.586	3.579
3	$^{22}Ne^* - ^{22}F^*$	3.144	3.127
3	$^{22}F^* - ^{22}O$	2.701	2.674

FIGURE CAPTIONS

Fig. 1. A schematic diagram of the electronic setup used in conjunction with the two counter particle identifier: only system 1 is shown in its entirety, system 2 being identical.

Fig. 2. Energy spectra of the reactions $^{26}Mg(p,t)^{24}Mg$ and $^{26}Mg(p,^{3}He)^{24}Na$ taken at $\theta_{lab} = 22.3°$ for 3200 μ Coulombs. The target was 99.2% enriched in ^{26}Mg. All peaks whose energies are marked (unbracketed) were used to establish calibration; see text.

Fig. 3. Energy spectra of the reactions $^{25}Mg(p,t)^{23}Mg$ and $^{25}Mg(p,^{3}He)^{23}Na$ taken at $\theta_{lab} = 24.1°$ for 970 μ Coulombs. The target was 91.5% enriched in ^{25}Mg. All peaks whose energies are marked (unbracketed) were used to establish calibration; see text.

Fig. 4. Angular distributions of the reactions $^{25}Mg(p,t)^{23}Mg$ and $^{25}Mg(p,^{3}He)^{23}Na$ leading to the $T = 3/2$ analogue states, the $(p,^{3}He)$ cross section having been multiplied by 0.92 to correct for kinematic effects. The angular distributions of the (p,t) reaction leading to the 5/2+,0.450 MeV state and to the 3/2+ ground state are also shown for comparison. The dashed curves are DWBA fits for the L values indicated, using the parameters given in Table 2.

Fig. 5. Energy spectra of the reactions $^{22}Ne(p,t)^{20}Ne$ and $^{22}Ne(p,^{3}He)^{20}F$ taken at $\theta_{lab} = 36.2°$ for 9280 μ Coulombs. The target was a 50:50 mixture of neon and methane, the neon being 92.0% enriched in ^{22}Ne. All peaks whose energies are marked were used to establish calibrations; see text.

Fig. 6. Energy spectra of the reactions $^{20}Ne(p,t)^{18}Ne$ and $^{20}Ne(p,^3He)^{18}F$ taken at $\theta_{lab} = 26.8°$ for 2570 μ Coulombs. The target was a 40:60 mixture of neon and methane, the neon being 99.9% enriched in ^{20}Ne. All peaks whose energies are marked (unbracketed) were used to establish calibrations; see text.

Fig. 7. Energy spectra of the reactions $^{21}Ne(p,t)^{19}Ne$ and $^{21}Ne(p,^3He)^{19}F$ taken at $\theta_{lab} = 22.3°$ for 4880 μ Coulombs. The neon target was enriched to 56.3% in ^{21}Ne, and included 21.1% ^{20}Ne and 22.6% ^{20}Ne. All peaks whose energies are marked were used to establish calibrations; see text.

Fig. 8. Angular distributions of the reactions $^{21}Ne(p,t)^{19}Ne$ and $^{21}Ne(p,^3He)^{19}F$ leading to the $T = 3/2$ analogue states, the $(p,^3He)$ cross section having been multiplied by 0.93 to correct for kinematic effects. The angular distributions of the reaction $^{21}Ne(p,t)^{19}Ne$, leading to the 4.013 MeV and ground states, as well as that of the reaction $^{20}Ne(p,t)^{18}Ne$ leading to the ground state, are shown for comparison. The dashed curves are DWBA fits for the L values indicated, using the parameters given in Table 2.

Fig. 9. A plot of the goodness of fit parameter (χ^2) versus the strength of A -dependence (λ) used in predicting Coulomb energy differences based on seniority and supermultiplet energy equations. The significance of the curves I, II, and III is discussed in section V of the text.

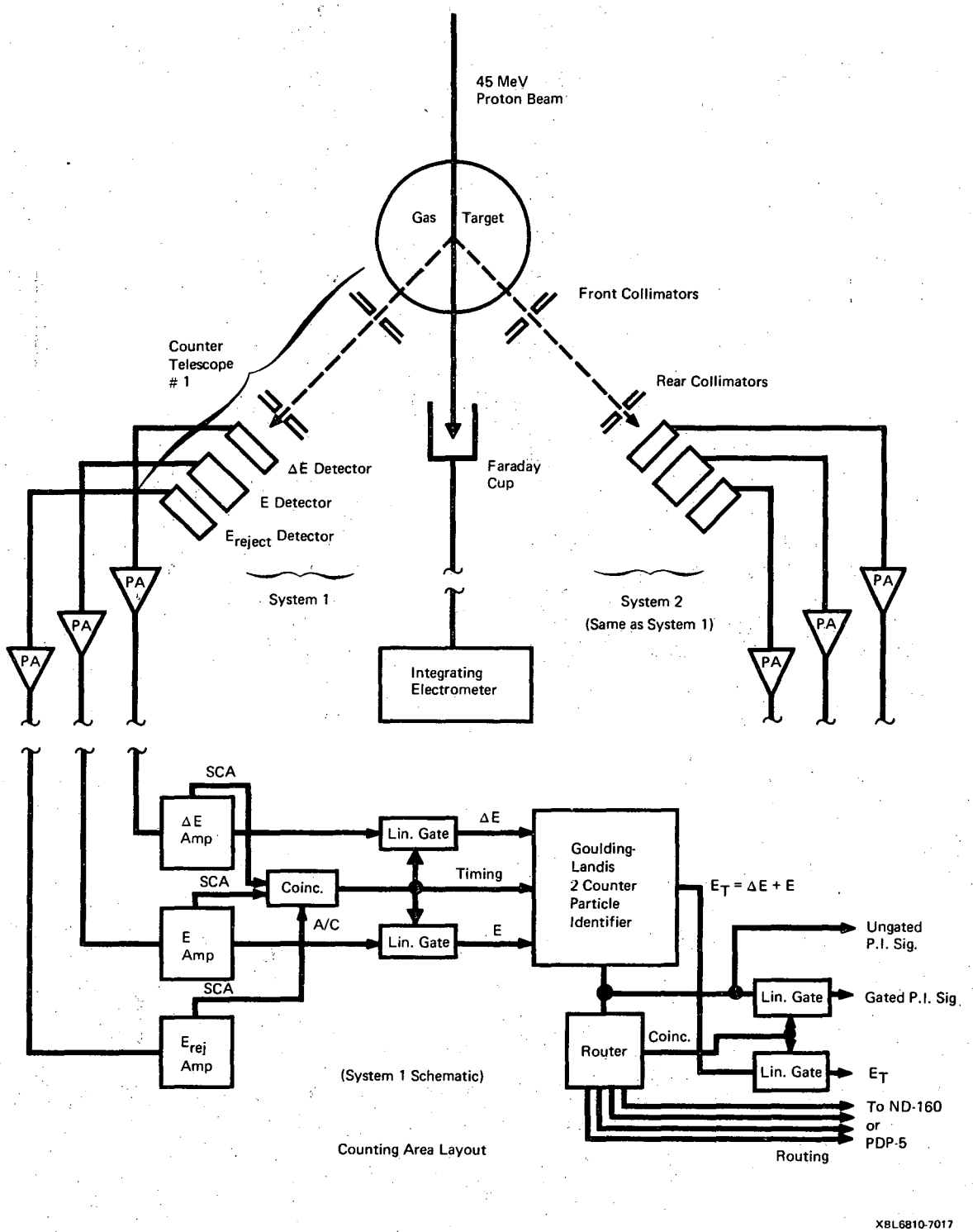
45 MeV
Proton Beam
Gas
Target
Front Collimators
Counter
Telescope
1
Rear Collimators
ΔE Detector
E Detector
E reject Detector
Faraday
Cup
PA
System 1
System 2
(Same as System 1)
Integrating
Electrometer
SCA
ΔE
Amp
Lin. Gate
ΔE
Goulding-
Landis
2 Counter
Particle
Identifier
Coinc.
Timing
E T = ΔE + E
A/C
E
Amp
Lin. Gate
E
Ungated
P.I. Sig.
Lin. Gate
Gated P.I. Sig
E rej
Amp
Router
Coinc.
Lin. Gate
E T
To ND-160
or
PDP-5
(System 1 Schematic)
Counting Area Layout
Routing
XBL6810-7017

Fig. 1

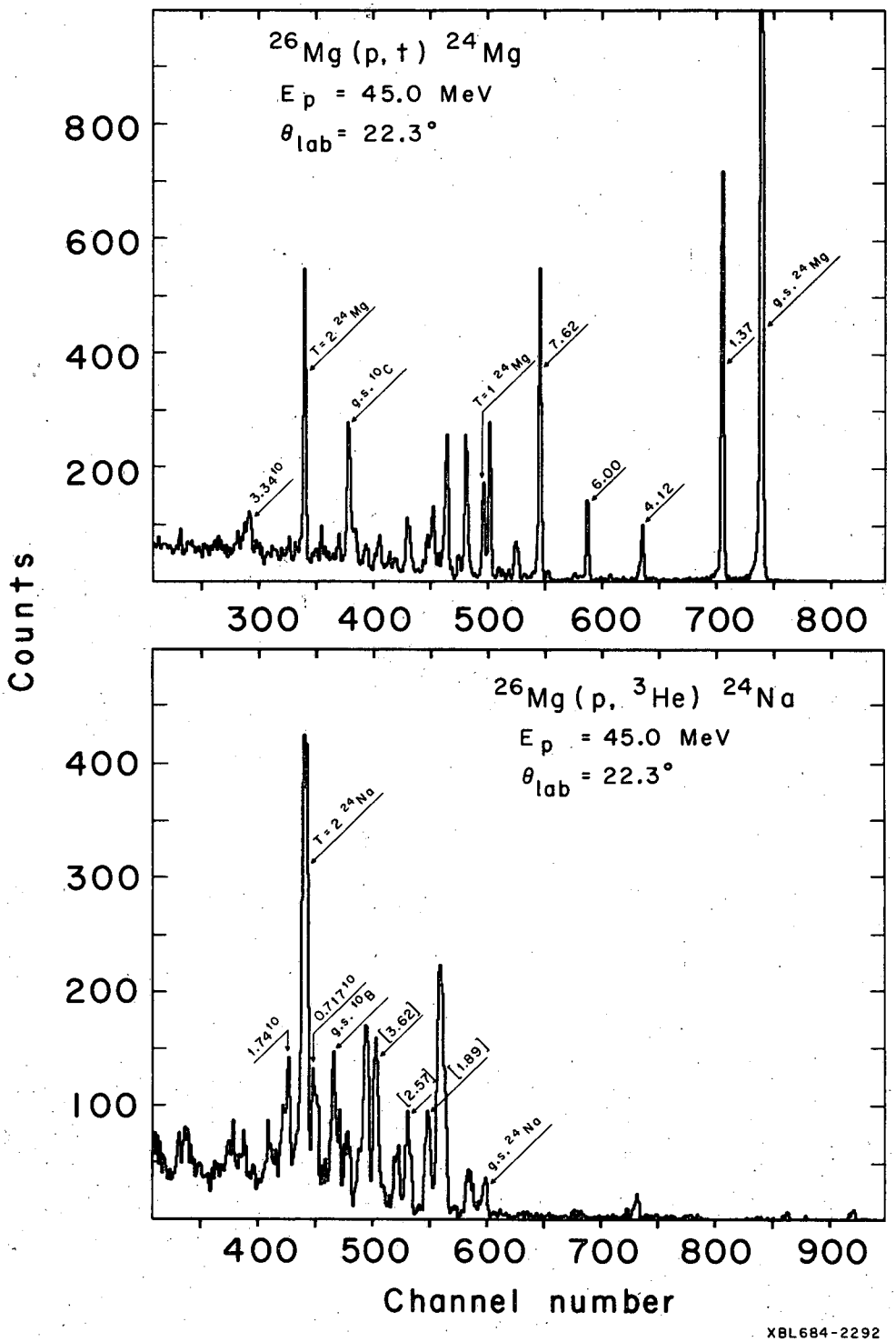
^{26}Mg (p, t) ^{24}Mg
E_p = 45.0 MeV
θ_{lab} = 22.3°
T=2 ^{24}Mg
g.s. ^{10}C
T=1 ^{24}Mg
7.62
6.00
4.12
1.37
g.s. ^{24}Mg
3.34 ^{10}
^{26}Mg (p, ^{3}He) ^{24}Na
E_p = 45.0 MeV
θ_{lab} = 22.3°
T=2 ^{24}Na
1.74 ^{10}
0.717 ^{10}
g.s. ^{10}B
[3.62]
[2.57]
[1.89]
g.s. ^{24}Na
Counts
Channel number
XBL684-2292

Fig. 2

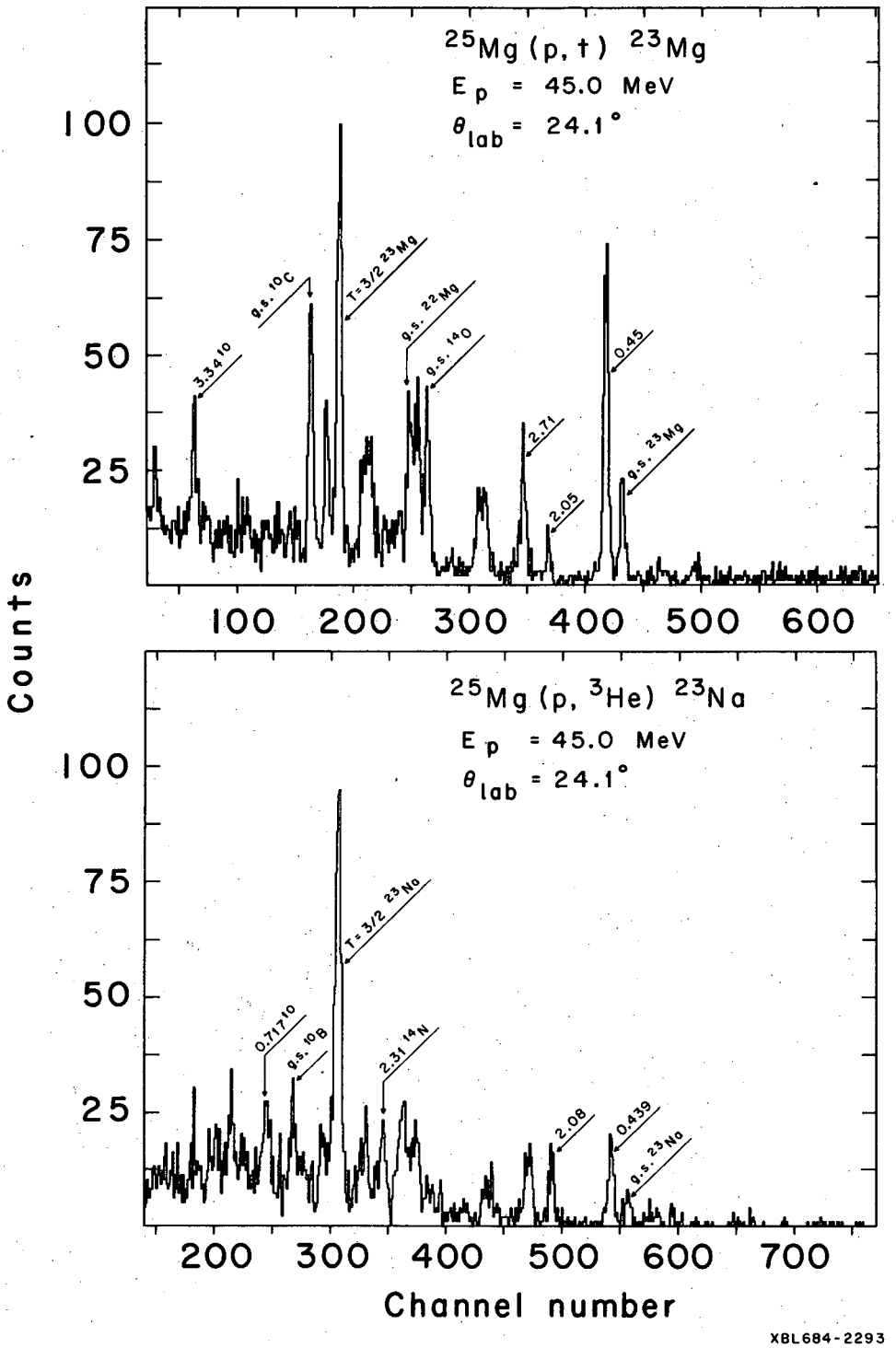
^{25}Mg (p, t) ^{23}Mg
E p = 45.0 MeV
θ lab = 24.1°
3.34 10
g.s. 10C
I=3/2 23Mg
g.s. 22Mg
g.s. 14O
2.71
2.05
0.45
g.s. 23Mg
^{25}Mg (p, 3He) ^{23}Na
E p = 45.0 MeV
θ lab = 24.1°
0.717 10
g.s. 10B
I=3/2 23Na
2.31 14N
2.08
0.439
g.s. 23Na
Counts
Channel number
XBL684-2293

Fig. 3

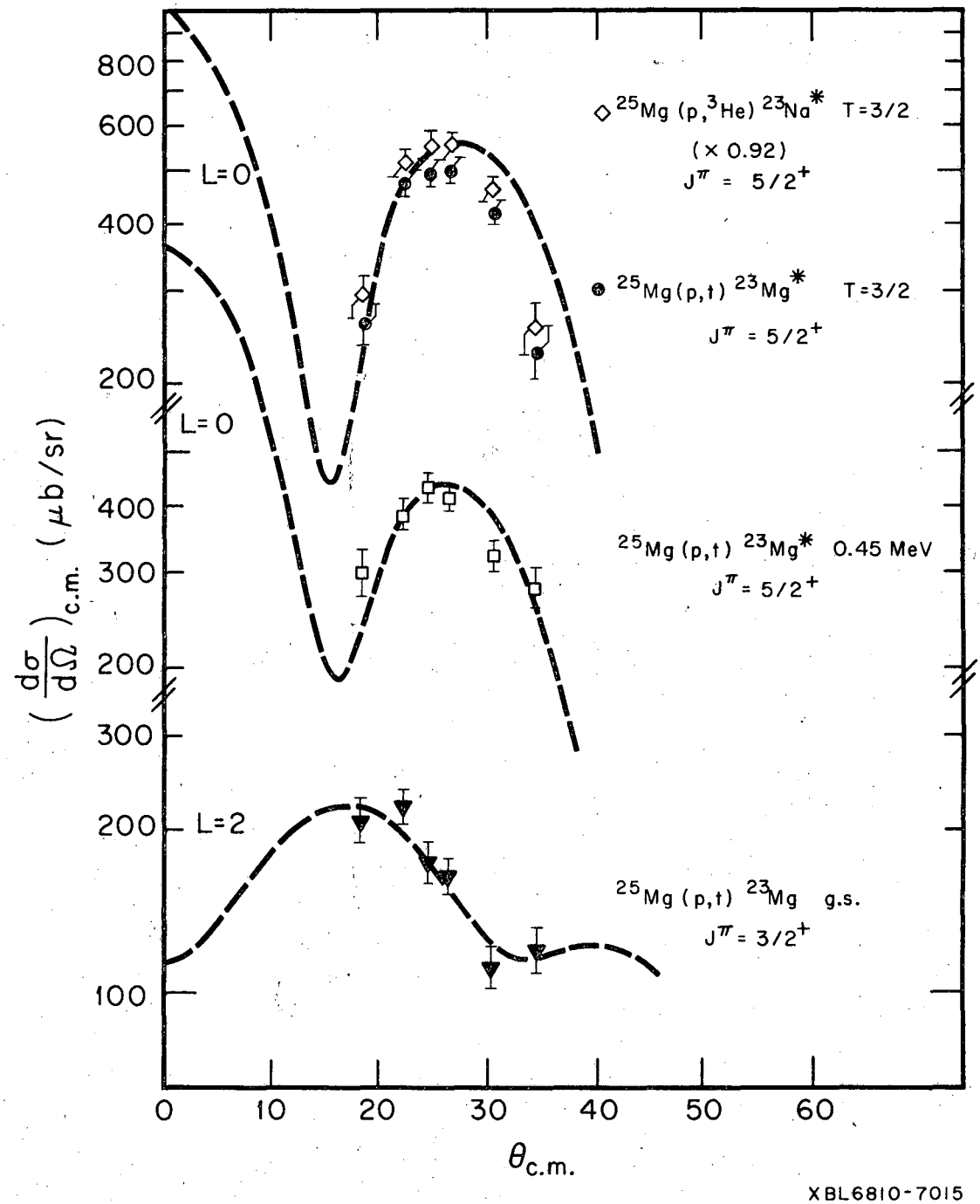
800
600
400
200
L=0
400
300
200
L=0
300
200
L=2
100
$\left(\frac{d\sigma}{d\Omega}\right)_{c.m.}$ (μb/sr)
◇ ^{25}Mg (p,^{3}He) ^{23}Na* T=3/2
(× 0.92)
J^{π} = 5/2^{+}
^{25}Mg(p,t) ^{23}Mg* T=3/2
J^{π} = 5/2^{+}
^{25}Mg (p,t) ^{23}Mg* 0.45 MeV
J^{π} = 5/2^{+}
^{25}Mg (p,t) ^{23}Mg g.s.
J^{π} = 3/2^{+}
0
10
20
30
40
50
60
$\theta_{c.m.}$
XBL6810-7015

Fig. 4

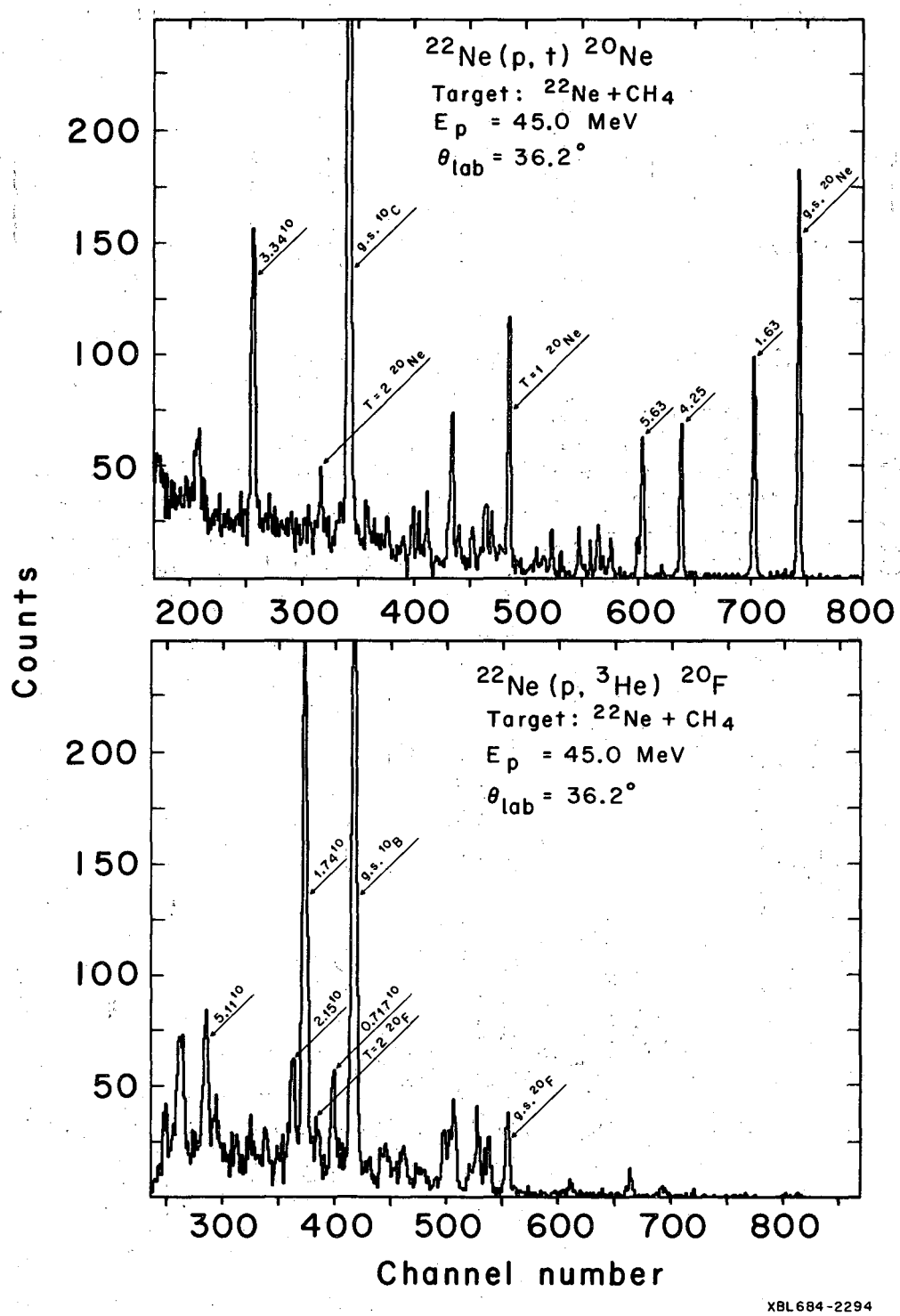
^{22}Ne (p, t) ^{20}Ne
Target: ^{22}Ne + CH$_4$
E_p = 45.0 MeV
θ_{lab} = 36.2°
3.34 ^{10}C
g.s. ^{10}C
T=2 ^{20}Ne
T=1 ^{20}Ne
5.63
4.25
1.63
g.s. ^{20}Ne
^{22}Ne (p, ^{3}He) ^{20}F
Target: ^{22}Ne + CH$_4$
E_p = 45.0 MeV
θ_{lab} = 36.2°
1.74 ^{10}B
g.s. ^{10}B
5.11 ^{10}C
2.15 ^{10}B
0.717 ^{10}B
T=2 ^{20}F
g.s. ^{20}F
Counts
Channel number
XBL684-2294

Fig. 5

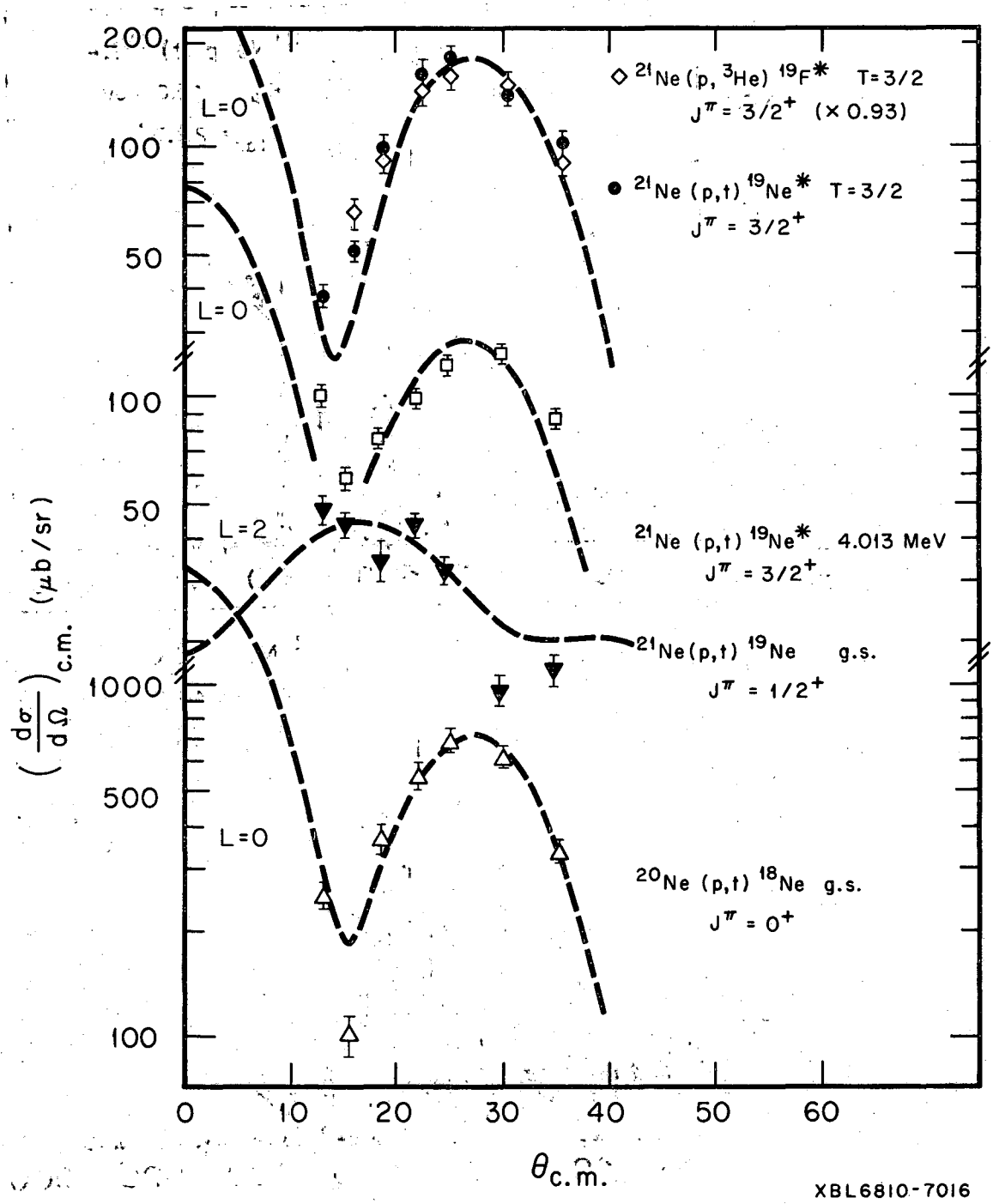
200
100
50
100
50
1000
500
100
L=0
L=0
L=2
L=0
◇ 21Ne (p, 3He) 19F* T=3/2
Jπ = 3/2+ (× 0.93)
● 21Ne (p,t) 19Ne* T=3/2
Jπ = 3/2+
21Ne (p,t) 19Ne* 4.013 MeV
Jπ = 3/2+
21Ne(p,t) 19Ne g.s.
Jπ = 1/2+
20Ne (p,t) 18Ne g.s.
Jπ = 0+
(dσ/dΩ)c.m. (μb/sr)
0
10
20
30
40
50
60
θc.m.
XBL6810-7016

Fig. 8

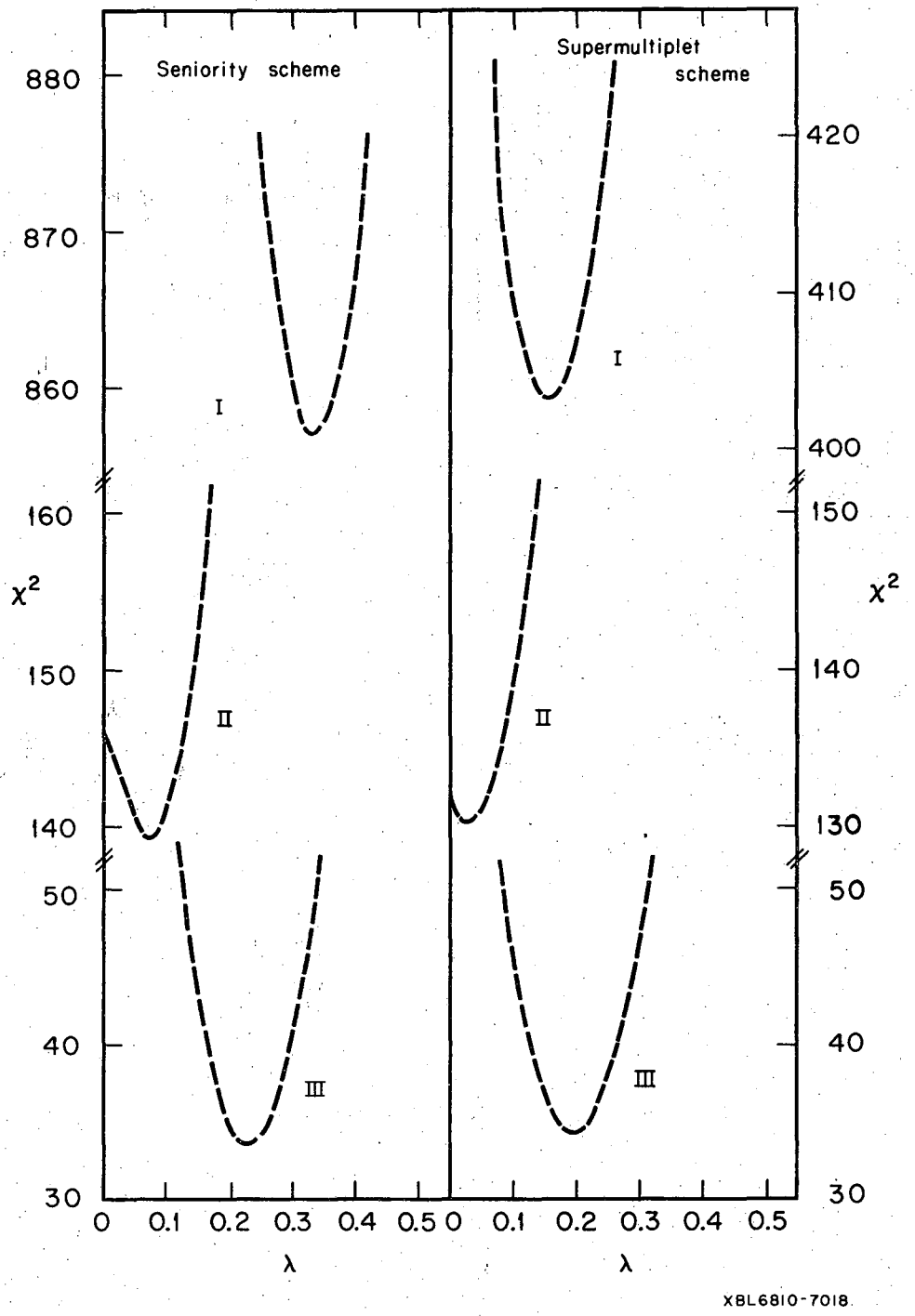
Seniority scheme
Supermultiplet scheme
880
870
860
160
150
140
50
40
30
420
410
400
150
140
130
50
40
30
I
II
III
χ^2
0 0.1 0.2 0.3 0.4 0.5
λ
XBL6810-7018

Fig. 9

LEGAL NOTICE

TECHNICAL INFORMATION DIVISION
LAWRENCE RADIATION LABORATORY
UNIVERSITY OF CALIFORNIA
BERKELEY, CALIFORNIA 94720